

A biologically inspired collision detection algorithm using differential optic flow imaging

Mukul Sarkar^{1,2}, David San Segundo Bello¹, Chris van Hoof¹, Albert Theuwissen^{2,3}
¹imec, ²Delft university of technology, ³Harvest Imaging
Mukul.Sarkar@imec-nl.nl

Abstract—A differential CMOS image sensor to detect collision using 1D binary differential optical flow is presented. The algorithm is inspired by the insects’ use of image expansion for saccadic motion and flight landing. The proposed model is simpler in implementation than the conventional Hassenstein-Reichardt elementary motion detectors used in most collision detection models. The binary output for the optic flow is generated at the pixel level, reducing the need for digital hardware and simplifying the process of collision detection. The experimental results show that the collision detection algorithm can trigger as near as 2cm from the object, opening the possibility of using these algorithms in narrow path autonomous agent navigations.

I. INTRODUCTION

Reliable estimation of the time to collision between two moving objects is very important in many applications such as autonomous agent navigation or predictive crash sensors for autonomous safety systems. Currently existing non-biologically inspired collision avoidance systems use a CCD/CMOS camera and digital processing devices to detect the approaching object. Such a collision detection system is not suitable for compact real-time realizations as it requires too much of computations.

It is well known that flying insects are able to detect obstacles in their flying path efficiently with little computational power by using optic flow. Optic flow is the pattern of apparent motion of objects, surfaces, and edges in a visual scene caused by the relative motion between an observer and the scene. Optic flow usually contains information about self motion and distance to potential obstacles and thus it is very useful for navigation [1].

Figure 1 show an image of an approaching object of diameter D at a constant velocity V along the optical axis. The distance between the lens and the object is $d(t)$ while the focal length of the lens is f .

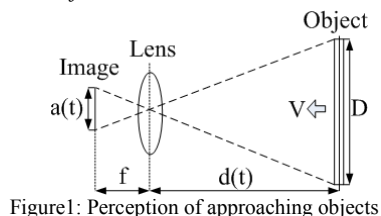


Figure1: Perception of approaching objects

The diameter of the obtained image and its derivative with respect to time is given as:

$$a(t) = \frac{f \times D}{d(t)} \quad [1]$$

The size image $a(t)$ in equation (1) increases with a decreasing distance $d(t)$ and vice versa. The change in the image size affects the optical flow perceived by the image sensor.

The most popular bio-inspired visual guided collision avoidance approach uses correlation-type elementary motion detector (EMD), first proposed by Hassenstein and Reichardt to compute the optic flow [2]. This model is very well established and often used in bio-inspired robots [3], [4], and [5]. The EMD correlates the response of one photoreceptor to the delayed response (inhibitory response) of an adjacent photoreceptor, both looking in the same direction. The transient response obtained by subtracting the two images is sensitive to temporal changes in the intensity of light and thus is relevant in motion detection of the objects. To retrieve the distance of the obstacle information, the optic flow from different regions of the visual field needs to be spatially integrated.

Existing implementations of the EMD use a complex circuit with many active and passive components in order to obtain the inhibition of the signal and the correlation. Additionally, the outputs of the EMD are not invariant to the changes in the background illumination and their responses are not only proportional to velocity changes but are strongly affected by the contrast and the spatial frequency components of the scene [6].

In order to have compact and low-power biologically inspired systems, the estimation of the optic flow has to be simplified. This means that rough qualitative properties of the optical flow are more desirable for efficient collision detection than accurate target distance estimation [1]. The collision avoidance maneuvers in insects can be explained in terms of perception of looming stimuli or expanding images. The landing behavior of insects and the saccade (rapid turns) exhibited by e.g. flies are believed to be triggered by image expansion as detected by an array of local motion detectors [5], [7]. Collision detection using expanding images is also relatively independent of the spatial structure of the object being approached.

This paper presents a differential CMOS image sensor to detect the collision using 1D binary optical flow. The aim is to design an efficient visual collision detection system, by in-pixel modulation of the image stored at various sampling times. This stored image is used to generate 1D binary optical flow which is spatially integrated by a row-wise counter.

Section II describes the designed image sensor to spatially integrate the generated binary 1D optic flow. Experimental

results are presented in section III and conclusions are presented in section IV.

II. SENSOR DESCRIPTION

A. Sensor architecture

Table 1 lists the sensor specifications and figure 2 shows the sensor architecture.

TABLE 1: Sensor specifications

Process	0.18 μ m 1P3M UMC CIS process
Active imager size	3.2 mm(H) x 3.2 mm(V)
Chip Size	4 mm(H) x 5 mm(V)
Active pixels	128 x 128
Pixel size	25 μ m x 25 μ m
Shutter type	Global shutter
Modes of operation	Double differential sampling (DDS) Differential imaging (DI)
Maximum data rate/master clock	64 MPS / 32 MHz
Supply voltage	1.8V

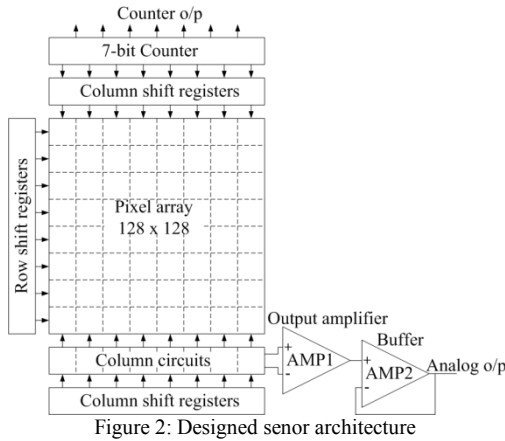


Figure 2: Designed sensor architecture

The chip is divided into four main blocks. The first one consists of the pixel array with the photodiodes and the associated circuitry for analog and digital computations. Second, placed below the pixel array is the analog readout circuit, consisting of column level circuits (double differential sampling circuit, DDS), an output amplifier, a buffer and the column shift register. Third, placed at the top is the digital readout circuit including a 7-bit counter to count the number of active high pixels in each row and a column shift register. Finally, the left side is dedicated to a row select logic and timing control blocks to address each row of pixels sequentially.

B. Pixel architecture

Each pixel contains a pinned photodiode, an analog comparator, two banks of analog memories and two SRAMs for digital memory. A simplified pixel diagram is shown in the figure 3.

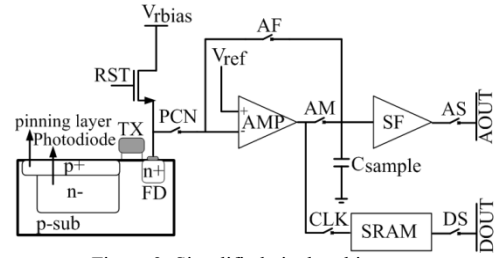


Figure 3: Simplified pixel architecture

The image capture begins with a reset of the pixel by closing the RST switch. The voltage at the floating diffusion node (FD) is then set to the reset voltage V_{rbias} . After opening the reset switch, the photodiode starts accumulating the photo-generated charge. The time spent accumulating charge is referred to as integration time or frame time. At the end of the integration time, the accumulated charge is transferred to the FD by closing the transfer gate switch TX .

The voltage change at the FD node due to the transferred photo-charge is sampled onto one of the two available sampling capacitors C_{sample} when the switch AM is closed. The source follower SF loads the column bus $AOUT$ via the analog row selection switch AS with the signal sampled on the sampling capacitor during readout of the pixel.

After the image is captured, the photodiode is disconnected from the processing elements using the switch PCN . The analog signal on C_{sample} is compared with a reference voltage V_{ref} , when the switch AF is closed, by using the amplifier AMP as a comparator. The resulting binary data is stored in the $SRAM$ when the switch CLK is closed. Two such $SRAMs$ are available to store the binary data of the two sampling capacitors. The switch DS loads the column bus $DOUT$ with the binary value stored in the $SRAM$.

C. Digital signal chain

The simplified digital signal chain is shown in Figure 4. In the digital signal chain, the binary data from the two $SRAMs$ is loaded onto the digital column bus $DOUT$. A 7-bit counter counts the number of active high pixels in each row. The outputs of the counter and the digital output are buffered out to the chip output pins.

D. Sensor performance

The prototype CMOS image sensor is implemented as shown in figure 5.

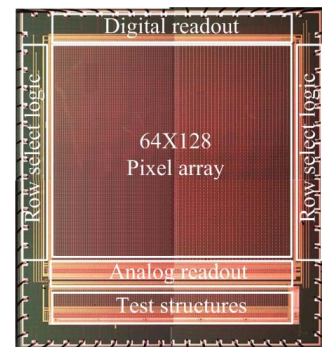


Figure 5: Die photograph of the designed image sensor

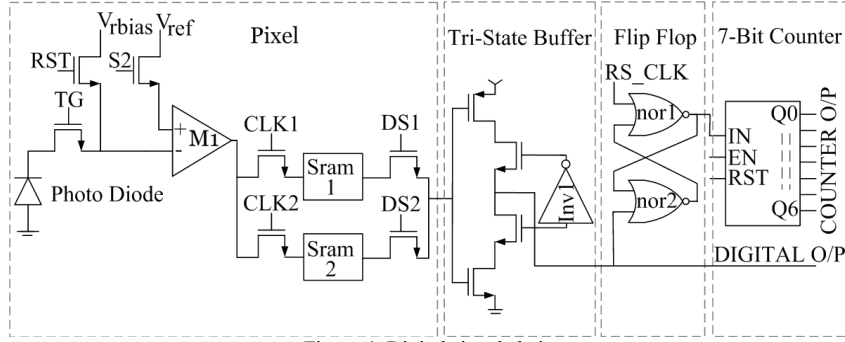


Figure 4: Digital signal chain

The sensor was quantitatively tested for conversion gain, sensitivity, dark current, dynamic range and SNR. The main measured performance parameters of the image sensor are summarized in table 2.

TABLE 2: Sensor performance characteristics

Parameters	Measured
Sensitivity	13.94 mV/ms
SNR	33 dB
Conversion gain	11.3 $\mu\text{V}/e^-$
Read Noise (CDS)	18 e^- at pixel level
Dark Current @ RT	18pA/cm ²
Dynamic Range (CDS)	68 dB at pixel level
Sense Node Cap.	14.5 fF
Full well	43186 e^-

III. COLLISION DETECTION

In the collision detection experiments, the image sensor is held stationary so that the optical flow is always generated by the motion of the object in the visual field. Figure 6 shows the variation in the light spot (approaching object). As the object approaches the image sensor, the spot size increases. Figure 6 also shows the algorithm used for the generation of differential optical flow.

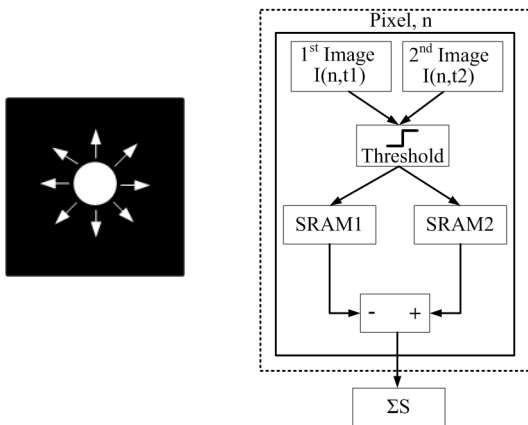


Figure 6: (left) Increasing spot size with approaching object and (right) collision detection model

The differential image is generated by the partial charge transfer [8], where the integrated charge at the photodiode capacitance is transferred to the FD node multiple times in one

frame. The differential image of the two spatially integrated digital images obtained from the $SRAM1$ and $SRAM2$ was computed off chip for this version of the sensor.

From the digital images, the percentage of active high pixels for a given illumination condition which is given by the ratio of total active high pixel to the total number of pixels in the array can be computed as:

$$\% \text{ of Active High Pixels} = \frac{\text{Total Active Pixels}}{\text{Total Number Of Pixels}} \quad [2]$$

Equation (2) represents the 1D binary optic flow. The percentage of the active high pixels will increase with the approaching object as predicted by equation (1). The variation in the percentage of active high pixels with the variation in the distance of the light source for single image capture is shown in figure 7. It shows that when the light source approaches the image sensor, the optic flow, which is the variation in the intensity with motion, causes more pixels to become active thus increasing the percentage of active high pixels.

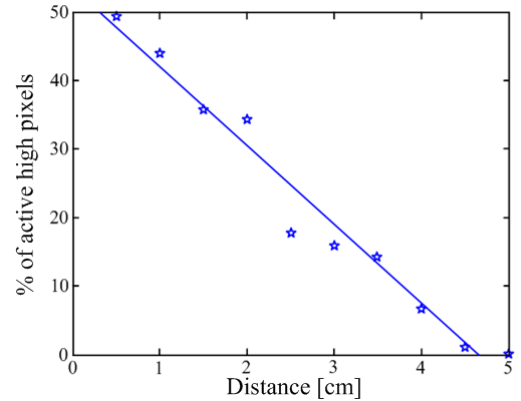


Figure 7: 1D optic flow variation with approaching object

The temporal decorrelation of the optic flow obtained using the partial charge transfer is shown in figure 8. The figure shows the variation in the percentage of active high pixels of two image captures for varying distance of the object from the imager. The first image is captured after an integration time of T_1 and the second after the total frame time FT . The modulation of the time instances allows to generate varying decorrelated 1D binary optical flow.

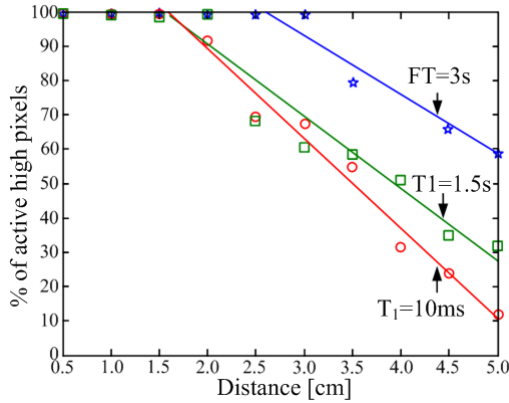


Figure 8: Temporally decorrelated optical flow with approaching objects.

The difference of the two temporally decorrelated optic flows is plotted in the figure 9. It can be observed that as object moves towards the image sensor, it has a certain threshold of percentage of pixels with changed states below which the object is very near to collision. In this case the collision detection mechanism does not need to use dedicated motion processing blocks. The collision can be detected to a very good degree of reliability using the percentage of changed pixels with the varying 1D differential optical flow.

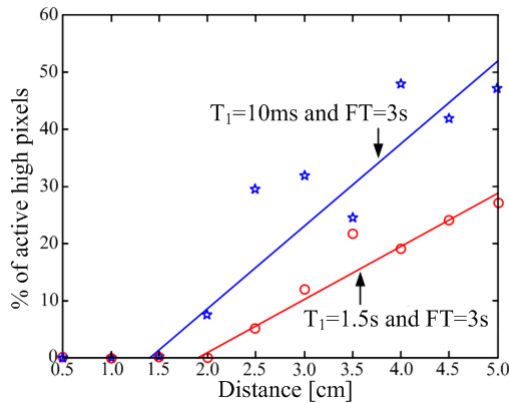


Figure 9: Temporal differential decorrelated optic flow for approaching object

The standard output of a collision detector using an EMD is a response which stays low when the object is far enough and peaks before collision for an approaching object and then collapses to low values again. The peaking of the collision detection algorithm depends on the delay in the delaying channel and the time an object takes to appear in the neighboring channel as well as the variations in the background illuminations. Thresholding of this response to ascertain collision is thus difficult.

Harrison [4] uses a collision detection algorithm based on the basic EMD model and the algorithm peaks at 230ms for an object with a velocity of 17cm/s. Thus the collision alert is generated at a distance of approx. 4cm. Similar method used by [3] produces an collision detection alert at a distance of 63m. The differential optical flow is shown to generate a collision alert for distances less than 2cm.

TABLE 3: Performance comparison

	[3]	[4]	This work
Method used	EMD model based on locust	Delay and correlate EMD	Differential optical flow imaging
Collision alert distance	63m	~ 4cm	< 2cm

Furthermore the proposed algorithm doesn't suffer from the inherent disadvantage of the EMD model of the accurate detection of the output peak, the output of the differential optical flow continues to stay low near collision allowing thresholding and thus is more stable. By modulating the differential time, it would be possible to prevent collision in very narrow paths thus helping navigation for the autonomous agents.

IV. CONCLUSION

We have presented a CMOS image sensor operating in temporal differential mode and spatial integration of 1D binary optic flow to detect collision of moving objects. The binary optical flow is generated in-pixel from multiple images stored in the in-pixel memories and spatially integrated using a counter. The computations are relatively easy and experimental results show the ability to detect collision with the approaching object as near as 2cm. This method allows the design of simple, miniaturized, low power and narrow path autonomous navigating agents.

ACKNOWLEDGMENT

The authors would like to thank DALSA for providing the test table to characterize the sensor, INVOMECA for helping with the fabrication of the chip, A. Mierop of DALSA, G. Meynants of CMOSIS and P. Merken for their valuable contributions to the project.

REFERENCES

- [1] M.V. Srinivasan, S.W. Zhang, J.S. Chahl, E. Barth, and S. Venkatesh, "How honeybees make grazing landings on flat surfaces". *Biological Cybernetics*, 83: pp. 171-183, 2000.
- [2] W. Reichardt, "Autocorrelation, a principle for the evaluation of sensory information by the central nervous system". *Sensory communications*, pp. 303-317, Wiley, New York, 1961.
- [3] H. Okuno and T. Yagi, "Bio-Inspired real-Time Robot Vision for Collision Avoidance". *Journal of Robotics and Mechanronics*, Vol. 20, No. 1, pp. 68-74, 2008
- [4] R. R. Harrison, "A biologically Inspired Analog IC for Visual Collision Detection". *IEEE Tran. on Circuits and Systems-I*, Vol. 52, No. 11, pp. 2308-2318, 2005.
- [5] M. B. Reiser and M. H. Dickinson, "A test bed for insect-inspired robotic control". *Philosophical Transactions: Mathematical, Physical & Engineering Sciences*, 361: pp. 2267-2285, 2003.
- [6] H.G. Krapp, "Neuronal matched filters for optic flow processing in flying insects". *Neuronal Processing of Optic Flow*, pp. 93-120. San Diego: Academic Press, 2000.
- [7] D.N. Lee, "A theory of visual control of braking based on information about time-to-collision". *Perception*, 5: pp. 437-459, 1976.
- [8] S. Shafie, S. Kawahito, I.A. Halin and W.Z.W.Hasan, "Non-linearity in wide dynamic range CMOS image sensors utilizing a partial charge transfer technique". *Sensors*, 9, pp. 9452-9467, 2009.